

Surface Impedance Boundary Conditions for the Finite Integration Technique

Sergey Yuferev¹, Luca Di Rienzo², and Nathan Ida³, *Fellow, IEEE*

¹Nokia Corporation, Tampere FIN-34101, Finland

²Dipartimento di Elettrotecnica, Politecnico di Milano, 32-20133 Milano, Italy

³Department of Electrical Engineering, The University of Akron, Akron, OH 44325-3904 USA

Approximate time-domain relations between the electric field integrated along the edge and the magnetic flux density integrated over the facet of the computational cell at the dielectric/conductor interface are derived and implemented into the finite integration technique to accurately eliminate the conducting region from the computational mesh. Both Cartesian and tetrahedral grids are considered. A numerical example is included to illustrate the method.

Index Terms—Differential forms, finite integration technique (FIT), surface impedance boundary condition.

I. INTRODUCTION

THE surface impedance concept has proven an efficient tool in computational electromagnetics. It provides approximate relations between the parameters of the electromagnetic field at the surface of the conductor. Thus, the conducting region does not need to be included in the mesh and can be “replaced” by surface impedance boundary conditions (SIBCs) in the numerical procedure. Originally SIBCs were developed in terms of the electric and magnetic field intensities, so they have been naturally implemented and widely used with the method of moments, the finite-difference time-domain (FDTD) method, and the node-based finite-element method.

In the past ten years, alternative formulations employing circulations and fluxes as state variables have gained acceptance. In particular, the “sister” method to the FDTD method is the finite integration technique (FIT) [1], and in both methods staggered dual grids are used for approximation of the electric- and magnetic-related parameters. Both the FDTD method and FIT are currently widely used to model high-frequency electromagnetic problems. FDTD-SIBC formulations have also become very popular [2]–[5], but the coupling of SIBCs and FIT does not seem to have been done. One possible reason is that the FIT requires SIBCs being represented in terms of the electric field integrated along the edge of the computational cell and the magnetic flux density integrated over the facet (differential 1- and 2-forms, respectively [6]). Thus, the purpose of this paper is derivation of time-domain SIBCs in terms of state variables used in FIT for Cartesian and tetrahedral grids.

II. TIME-DOMAIN SURFACE IMPEDANCE CONCEPT

Consider a homogeneous body of finite conductivity surrounded by a nonconductive medium and illuminated by a pulsed electromagnetic field. Let the time variation of the incident field be such that the electromagnetic penetration depth δ

into the body remains small compared with the characteristic dimension D of the surface of the body

$$\delta = \sqrt{\tau/\sigma\mu} \ll D \quad (1)$$

where τ is the incident pulse duration, and σ and μ are conductivity and permeability of the body, respectively. It means that the conducting region is so large that the wave attenuates completely inside the region. Then, the electromagnetic field distribution in the conductor’s skin layer can be described as a damped plane wave propagating in the bulk of the conductor normal to its surface. In other words, the behavior of the electromagnetic field in the conducting region may be assumed to be known *a priori*. The electromagnetic field is continuous across the real conductor’s surface so the intrinsic impedance of the wave remains the same at the interface. Therefore, the relations between tangential (x - and y -) components of the electric field E and magnetic flux density B or normal (z -) and tangential (x - and y -) components of the magnetic flux density at any point of the conductor/dielectric interface can be written in the form [7]

$$E_x = (\mu\varepsilon)^{-1/2} \frac{\partial}{\partial t} (B_y * T) = (\mu\varepsilon)^{-1/2} B_y * \tilde{T} \quad (2a)$$

$$E_y = -(\mu\varepsilon)^{-1/2} \frac{\partial}{\partial t} (B_x * T) = -(\mu\varepsilon)^{-1/2} B_x * \tilde{T} \quad (2b)$$

$$B_z = (\varepsilon\mu)^{-1/2} \nabla \cdot [(\vec{n} \times \vec{B}) \times \vec{n}] * T \quad (3)$$

where time-domain functions T and \tilde{T} are defined as

$$T(t) = \exp\left(-\frac{\sigma t}{2\varepsilon}\right) I_0\left(\frac{\sigma t}{2\varepsilon}\right) \quad (4)$$

$$\tilde{T}(t) = \delta(t) + \frac{\sigma}{2\varepsilon} \left[I_1\left(\frac{\sigma t}{2\varepsilon}\right) - I_0\left(\frac{\sigma t}{2\varepsilon}\right) \right] \exp\left(-\frac{\sigma t}{2\varepsilon}\right) \quad (5)$$

and where I_n is the n -order modified Bessel function.

The conditions in (2) and (3) are of the Leontovich order of approximation. Note that they are the first nonzero terms in the asymptotic expansions representing *high-order* SIBCs [7].

III. FIT

The example of the orthogonal dual mesh used in FDTD and FIT is shown in Fig. 1. In FDTD, the nodes, where electric and magnetic fields are calculated, are located at the middle of edges

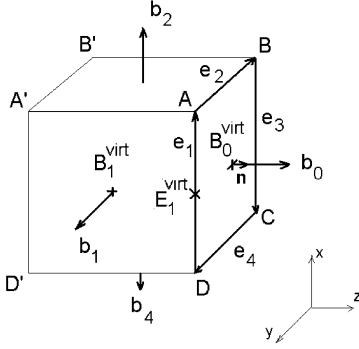


Fig. 1. Cartesian computational cell used in the FIT and FDTD method.

and in the middle of facets, respectively. In FIT, state variables are the so-called grid voltages and grid fluxes related with edges and facets [1]

$$e = \int_{L_e} \vec{E} \cdot d\vec{l}; \quad h = \int_{L_h} \vec{H} \cdot d\vec{l} \quad (6a)$$

$$d = \iint_{S_d} \vec{D} \cdot \vec{n} ds; \quad b = \iint_{S_b} \vec{B} \cdot \vec{n} ds. \quad (6b)$$

Here, L_i and S_i are the cell's edge and facet, respectively, and the vectors $d\vec{l}$ and \vec{n} are directed along the edge and normal to the facet, respectively.

Faraday's law in integral form applied to the facet ABCD of the computational cell shown in Fig. 1 can be written with variables (6) as follows:

$$e_1 + e_2 + e_3 + e_4 = db_0/dt. \quad (7)$$

Material relations between e and d are obtained by introduction of a virtual continuous component E^{virt} at the intersection point of the dual and primary grids [1]. Since the normal vector to the dual facet is collinear with the direction of the intersecting primary edge, one obtains

$$d = \varepsilon E^{\text{virt}} S_d; \quad e = E^{\text{virt}} L_e. \quad (8a)$$

Similarly, a virtual magnetic flux density B^{virt} is allocated as a continuous normal component at the center of the primary facet so that

$$b = B^{\text{virt}} S_b; \quad h = \mu^{-1} B^{\text{virt}} L_h. \quad (8b)$$

IV. SIBC-FIT FORMULATION FOR CARTESIAN GRIDS

Suppose facet ABCD of the cell shown in Fig. 1 belongs to the dielectric/conductor interface. To truncate the mesh, additional equations relating e_1, e_2, e_3, e_4 , and b_0 and containing material properties of the conductor are needed.

Performing integration on both sides of (3) over the facet ABCD and applying vector identities, we obtain

$$\begin{aligned} b_0 &= \iint_{S_{b_0}} (\vec{B})_z ds \\ &= T * \frac{1}{\sqrt{\varepsilon\mu}} \iint_{S_{b_0}} \nabla \cdot [(\vec{n} \times \vec{B}) \times \vec{n}] ds \\ &= -T * \frac{1}{\sqrt{\varepsilon\mu}} \iint_{S_{b_0}} \vec{n} \cdot \nabla \times (\vec{n} \times \vec{B}) ds \end{aligned} \quad (9)$$

where the quantity \vec{B} is assigned to the facet ABCD.

Application of Stoke's theorem to the last equation yields

$$\begin{aligned} b_0 &= -T * \frac{1}{\sqrt{\varepsilon\mu}} \oint_L (\vec{n} \times \vec{B}) \cdot d\vec{l} \\ &= -T * \frac{1}{\sqrt{\varepsilon\mu}} \sum_{k=1}^4 \int_{L_k} (\vec{n} \times \vec{B}) \cdot d\vec{l}. \end{aligned} \quad (10)$$

From Fig. 1, it follows that

$$\vec{n} \times \vec{B} \Big|_{ABCD} = -B_y \vec{a}_x + B_x \vec{a}_y \quad (11)$$

where \vec{a}_x, \vec{a}_y and \vec{a}_z are unit vectors of the global Cartesian coordinate system shown in Fig. 1 and $\vec{n} = \vec{a}_z$. Substituting (11) into (10) and taking into account that

$$\begin{aligned} d\vec{l}_{DA} &= dl_{DA} \cdot \vec{a}_x; \quad d\vec{l}_{AB} = -dl_{AB} \cdot \vec{a}_y \\ d\vec{l}_{BC} &= -dl_{BC} \cdot \vec{a}_x; \quad d\vec{l}_{CD} = dl_{CD} \cdot \vec{a}_y \end{aligned}$$

we obtain

$$\left. \begin{aligned} \int_{L_{DA}} (\vec{n} \times \vec{B}) \cdot d\vec{l} &= - \int_{L_{DA}} (\vec{B}_{DA})_y dl_{DA} = -B_1^{\text{virt}} L_{e1} = -\frac{L_{e1}}{S_{b1}} b_1 \\ \int_{L_{AB}} (\vec{n} \times \vec{B}) \cdot d\vec{l} &= - \int_{L_{AB}} (\vec{B}_{AB})_x dl_{AB} = -B_2^{\text{virt}} L_{e2} = -\frac{L_{e2}}{S_{b2}} b_2 \\ \int_{L_{BC}} (\vec{n} \times \vec{B}) \cdot d\vec{l} &= \int_{L_{BC}} (\vec{B}_{BC})_y dl_{BC} = -B_3^{\text{virt}} L_{e3} = -\frac{L_{e3}}{S_{b3}} b_3 \\ \int_{L_{CD}} (\vec{n} \times \vec{B}) \cdot d\vec{l} &= \int_{L_{CD}} (\vec{B}_{CD})_x dl_{CD} = -B_4^{\text{virt}} L_{e4} = -\frac{L_{e4}}{S_{b4}} b_4 \end{aligned} \right\} \quad (12)$$

where

$$\begin{aligned} L_{e1} &= DA, \quad L_{e2} = AB, \quad L_{e3} = BC, \quad L_{e4} = CD, \\ S_{b1} &= S_{DAA'D'}, \quad S_{b2} = S_{ABB'A'}, \\ S_{b3} &= S_{BCC'B'}, \quad S_{b4} = S_{CDD'C'}. \end{aligned}$$

Substitution of (12) into (10) yields the SIBC (3) in variables of FIT

$$b_0 = T * \frac{1}{\sqrt{\varepsilon\mu}} \sum_{k=1}^4 \frac{L_{ek}}{S_{bk}} b_k. \quad (13)$$

Substituting (13) into the Faraday law (7) we obtain the analog of (2)

$$e_k = \frac{1}{\sqrt{\varepsilon\mu}} \frac{L_{ek}}{S_{bk}} \frac{\partial}{\partial t} (T * b_k) = \frac{1}{\sqrt{\varepsilon\mu}} \frac{L_{ek}}{S_{bk}} (\tilde{T} * b_k). \quad (14)$$

The relations in (13) and (14) are the desired SIBCs in terms of circulation of the electric field and magnetic flux.

V. SIBC-FIT FORMULATION FOR TETRAHEDRAL GRIDS

The conditions in (13) and (14) can be generalized for tetrahedral grids. Let facet ABC of the tetrahedron, shown in Fig. 2, be a part of the conductor/dielectric interface.

In this case, the SIBCs can be written in the form:

$$\begin{aligned} b_{ABC} &= \frac{1}{\sqrt{\mu\varepsilon}} T * \sum_{k=1}^3 \frac{L_{ek}}{S_{bk}} b_k \sin \phi_k, \quad k = 1, 2, 3 \\ e_k &= \frac{1}{\sqrt{\mu\varepsilon}} \frac{L_{ek}}{S_{bk}} \sin \phi_k \frac{\partial}{\partial t} (b_k * T) = \end{aligned} \quad (15)$$

$$= \frac{1}{\sqrt{\mu\varepsilon}} \frac{L_{ek}}{S_{bk}} \sin \phi_k b_k * \tilde{T} \quad (16)$$

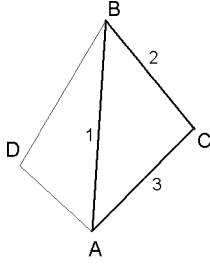


Fig. 2. Tetrahedral computational cell.

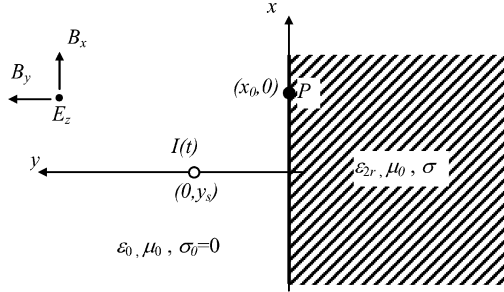


Fig. 3. Geometry of the test problem.

where $b_1 = b_{ABD}$, $b_2 = b_{BCD}$, $b_3 = b_{ACD}$, $L_{e1} = AB$, $L_{e2} = BC$, $L_{e3} = CD$, $S_{b1} = S_{ABD}$, $S_{b2} = S_{BCD}$, $S_{b3} = S_{ACD}$; ϕ_1 is the angle between facets ABC and ABD , ϕ_2 is the angle between facets ABC and BCD , and ϕ_3 is the angle between facets ABC and ACD .

VI. NUMERICAL EXAMPLE

In order to test the formulation on a simple example, we considered the two-dimensional problem of a line current $I(t)$ placed at point $(0, y_s)$ radiating over a half-space (Fig. 3). The electric field was observed in point $(x_0, 0)$.

The field was computed by means of an FIT code. The computational domain was discretized into a 100×100 Cartesian grid made of one layer of three-dimensional Yee cubic cells with side length $\Delta = 0.015$ m. We implemented condition (13) over the interface, using recursive formulas given in [4] for the convolution. Mur's first-order absorbing boundary conditions were used at the other boundaries.

The following current pulse was considered (Fig. 4):

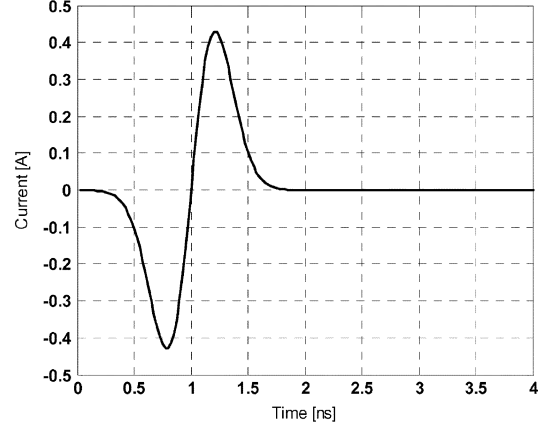
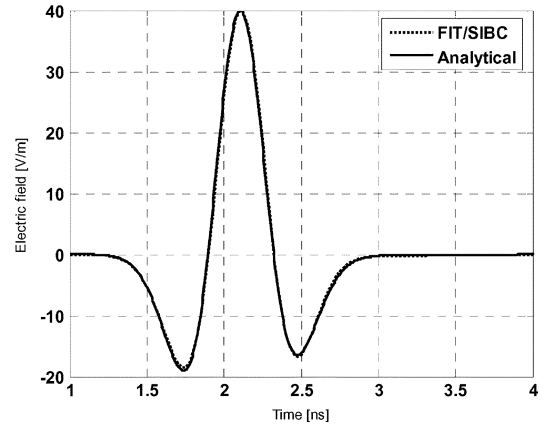
$$I(t) = \frac{t - \tau_0}{\tau} e^{-\left(\frac{t - \tau_0}{\tau}\right)^2} \quad (17)$$

with $\tau = 40\Delta t$, $\tau_0 = 12\Delta t$, where the time step Δt was chosen as $\Delta t = \Delta x / 2c_0$.

The computed results were compared with the exact solution of the problem in the time domain, obtained from the solution in the frequency domain reported in [2] by means of the inverse fast Fourier transform algorithm.

The Fourier transform of $I(t)$ in (17) was derived analytically

$$I(\omega) = -\frac{j\sqrt{\pi}}{2} \tau^2 \omega e^{-j\omega\tau_0} e^{-\frac{\omega^2\tau^2}{4}} \quad (18)$$

Fig. 4. Current pulse $I(t)$.Fig. 5. Electric field at the observation point for $y_s = 20\Delta$; $x_0 = 10\Delta$; $\sigma = 10$ S/m; $(k_p \delta_p)^2 = 0.0279$; $(\delta_p / y_s)^2 = 1.105e^{-4}$.

and then substituted in the expression of the electric field at the observation point [2]

$$E_z(\omega, x_0) = -\frac{c_0 \mu_0 k_0}{2\pi} I(\omega) \int_0^\infty \frac{2}{\sqrt{1 - \xi^2} + \sqrt{\epsilon_{2r} - \xi^2}} \cdot \exp(-jk_0 y_s \sqrt{1 - \xi^2}) \cos(k_0 x_0 \xi) d\xi \quad (19)$$

where $k_0 = \omega / c_0$.

Following [2] and [8], we described the problem using two parameters: $(k_p \delta_p)^2$ and $(\delta_p / y_s)^2$, where k_p is the wavenumber at the peak of the spectrum of the current pulse and δ_p is the skin depth also at the peak of the spectrum. The condition $(k_p \delta_p)^2 \ll 1$ assures we deal with a good conductor. The condition $(\delta_p / y_s)^2 \ll 1$ implies that within the conductor the variation of the electromagnetic field in directions along the surface is small compared to the variation in the normal direction so that the surface impedance concept can be applied [8]. Both conditions must be satisfied in order to obtain accurate results from the developed code, as in Figs. 5 and 6. Differences between the exact and the computed field were noted at low values of conductivity, as in Fig. 7, when $(k_p \delta_p)^2 > 1$.

The discussion of the computational saving when using SIBC for the case of FDTD can be found in [2]. Since FIT over Cartesian grid is computationally equivalent to FDTD, as shown in [1], the same analysis is valid here. More specifically, the presented numerical example was solved using 54 MB of

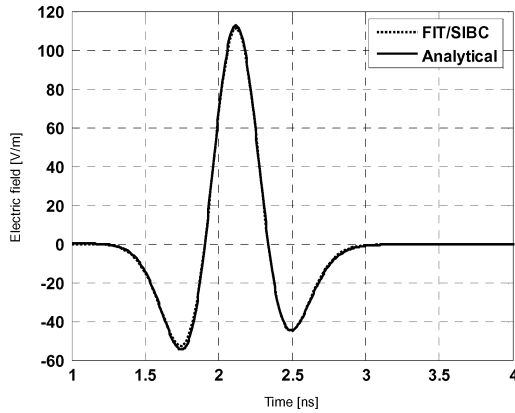


Fig. 6. Electric field at the observation point for $y_s = 20\Delta$; $x_0 = 10\Delta$; $\sigma = 1$ S/m; $(k_p \delta_p)^2 = 0.2796$; $(\delta_p / y_s)^2 = 0.0111$.

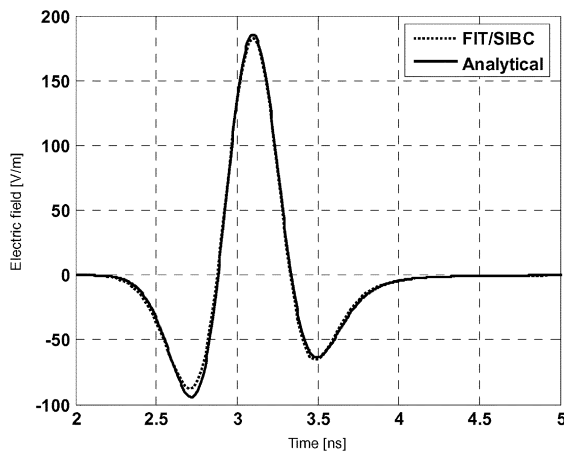


Fig. 7. Electric field at the observation point for $y_s = 40\Delta$; $x_0 = 10\Delta$; $\sigma = 0.1$ S/m; $(k_p \delta_p)^2 = 27.96$; $(\delta_p / y_s)^2 = 0.2763$.

memory and each time step was computed in 0.4375 s using a Pentium IV 1.8-GHz PC with 1.5-GB RAM.

VII. CONCLUSION

Time-domain SIBCs have been obtained in terms of circulation of the electric field and the magnetic flux. The proposed representation made possible natural implementation of SIBCs into the numerical techniques employing 2-forms as state variables for both Cartesian and tetrahedral elements.

REFERENCES

- [1] T. Weiland, "Advances in FIT/FDTD modeling," *Proc. 18th Ann. Rev. Progr. Appl. Computat. Electromagn.*, pp. 1.1–1.14, 2002.
- [2] J. G. Maloney and G. S. Smith, "The use of surface impedance concepts in the finite-difference time-domain method," *IEEE Trans. Antennas Propag.*, vol. 40, no. 1, pp. 38–48, Jan. 1992.
- [3] J. H. Beggs, R. J. Luebbers, K. S. Yee, and K. S. Kunz, "Finite-difference time-domain implementation of surface impedance boundary conditions," *IEEE Trans. Antennas Propag.*, vol. 40, no. 1, pp. 49–56, Jan. 1992.
- [4] K. S. Oh and J. E. Schutt-Aine, "An efficient implementation of surface impedance boundary conditions for the finite-difference time-domain method," *IEEE Trans. Antennas Propag.*, vol. 43, no. 7, pp. 660–666, Jul. 1995.
- [5] S. Yuferev, N. Farahat, and N. Ida, "Use of the perturbation technique for implementation of surface impedance boundary conditions for the FDTD method," *IEEE Trans. Magn.*, vol. 36, no. 4, pp. 2605–2608, Jul. 2000.
- [6] G. Deschamps, "Electromagnetics and differential forms," *Proc. IEEE*, vol. 69, no. 6, pp. 676–696, Jun. 1981.
- [7] S. Yuferev and N. Ida, "Time domain surface impedance boundary conditions of high order of approximation," *IEEE Trans. Magn.*, vol. 34, no. 5, pp. 2605–2608, Sep. 1998.
- [8] G. S. Smith, "On the skin effect approximation," *Amer. J. Phys.*, vol. 58, no. 10, pp. 996–1002, 1990.

Manuscript received June 20, 2005 (e-mail: luca.dirienzo@polimi.it).